A New Approach to Contacts and Rigid Body Interactions in LS-DYNA

Fredrik Bengzon[1], Thomas Borrvall[1], Anders Jonsson[1], Gert Petersen[2]

[1]DYNAmore Nordic AB, An Ansys Company

[2]LEGO Systems A/S

1 Introduction

Traditionally in LS-DYNA (almost) all contact definitions use a penalty formulation. This means that penetration in the contact is required to obtain a contact force between interacting entities. It is then up to the user to verify that the penetrations are small enough not to influence the results. The Mortar contacts [1], which have become the preferred choice for implicit analyses, is of penalty type.
Also, the rigid walls (***RIGIDWALL**) use a penalty method in implicit analyses. To find a good penalty stiffness setting may be problematic if solid elements (especially tetrahedra), or soft materials, such as rubber or plastic, are involved. It can be hard to find a good trade-off between reasonably small penetrations and implicit convergence.
In this paper, we present a new approach to rigid walls and rigid analytical shapes (***CONTACT_ENTITY**, see Fig.1) using an augmented Lagrange formulation [4] that enforces zero penetrations. The implementation is intended for implicit analyses. The rigid wall implementation is a re-formulation of the existing functionality, while the implementation of ***CONTACT_ENTITY** for implicit analysis is new.

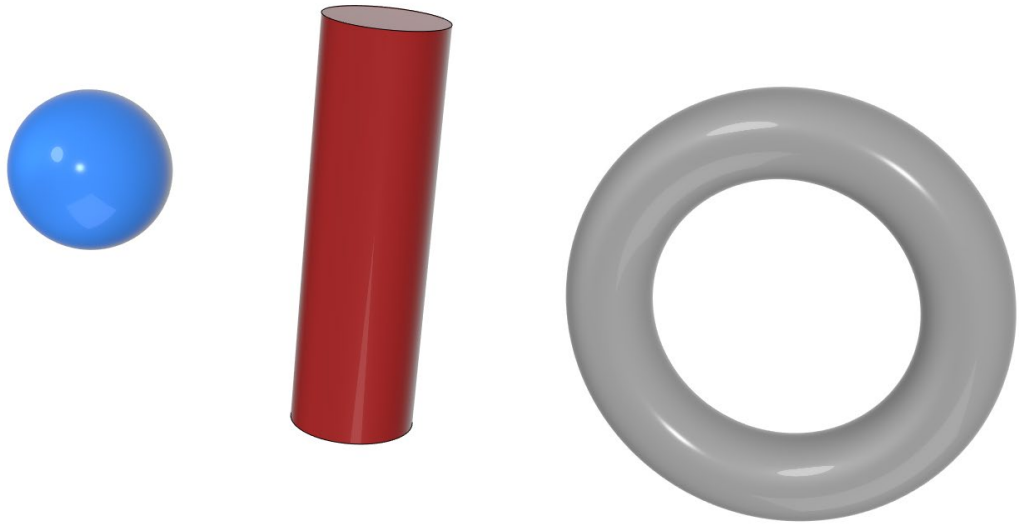

*Fig.1: Examples of pre-define analytical shapes that can be created by ***CONTACT_ENTITY**.*

We also present a new small-sliding contact algorithm dedicated to implicit analyses using the same approach. In many analysis applications where implicit is the dominating solution technique, for example static stress analyses and high cycle fatigue analyses, only small relative motions are expected between the parts in the model. For such analyses, small-sliding contact is sufficient, and the small-sliding assumption, meaning that the contact pairs need not to be updated after one initial contact search, simplifies the numerical implementation in many ways. This small-sliding, augmented Lagrange contact uses the keyword ***CONTACT_CONSTRAINT_SURFACE_TO_SURFACE** and is activated by the implicit accuracy ***IACC*** variable of ***CONTROL_ACCURACY**.
The use of Lagrange multiplies will rearrange the structure of the stiffness matrix, generating a saddle point problem. For this type of problem, the traditional quasi-Newton approach of BFGS in LS-DYNA is inefficient. As an alternative, methods of Jacobian-Free Newton-Krylov (JFNK) type [3] can be used to improve the nonlinear convergence, and the implementation is also outlined.

1.1 Acknowledgement

In this Paper, public FE-models of a 2010 Toyota Yaris [5][6] is used as a basis for some examples, see Sections 3.3 and 3.5. The work of the CCSA at the George Mason University is gratefully acknowledged.

2 Theoretical background

2.1 Augmented Lagrangian Contact Formulation

For ease of presentation let us consider the simplified situation of a rigid wall contacting a tracked surface. The rigid wall can be either a plane, a cylinder, a sphere, or a prism, while the tracked surface is a set of node points. Because of its simple shape it is easy to obtain geometric information such as normal, n, and tangent plane, t, of the rigid wall at any point. The distance between a tracked node and its projection, along the rigid wall normal, onto the rigid wall is the gap, g_N. A positive gap implies that the node is outside the rigid wall, while a zero gap means that the node and wall are in contact. Negative gaps are not allowed.

Let $\lambda_N \subset \mathbb{R}$ be the normal pressure for maintaining a closed gap between rigid wall and a contacting node. The conditions for normal contact can be succinctly summarized in the complementarity

$$g_N \geq 0, \quad \lambda_N \geq 0, \quad g_N \lambda_N = 0$$

This expresses impenetrability of the rigid wall, that is, the fact that either a gap or a normal pressure exists, but not both at the same time. Using the minimum map formula this is equivalent to the equation

$$h_N = \min(g_N, \lambda_N) = 0$$

Further, if a tracked node in contact with the rigid wall slips an amount g_T along the wall there will be friction forces. Such forces oppose any relative movement between node and wall and act in the plane t tangential to the wall. For Coulomb friction the tangential reaction forces, $\lambda_T \subset \mathbb{R}^2$, obey the equations

$$h_T = \lambda_T - \gamma(\lambda_T - g_T) = 0$$
$$\gamma = \frac{s}{\max(s, \|\lambda_T - g_T\|)}$$

where $s = \mu\lambda_N$ with $0 \leq \mu \leq 1$ the coefficient of friction. As long as the magnitude of the tangential forces is less than the threshold s no slip can occur and the wall and node will stick together. However, if this is not the case then there will be a sliding movement between them.

Collecting normal and tangential directions into the matrix $P = [n \quad t]$, and defining also the vectors

$$\lambda = \begin{bmatrix} \lambda_N \\ \lambda_T \end{bmatrix}, \quad h = \begin{bmatrix} h_N \\ h_T \end{bmatrix}$$

the translational force that needs to be added to each node on the tracked surface is given by

$$f = \kappa P(\lambda - h)$$

with $\kappa > 0$ is a scaling parameter for unit consistency.

We refer the reader to [4] and the references therein for a more thorough explanation of Augmented Lagrangian contacts and finite elements.

2.2 Jacobian-Free Newton-Krylov Method

The equations arising from finite element discretization are nonlinear and therefore solved using Newton's method. Its classical form is to iterate on the linearized system. Indeed, given some initial guess for the solution x_0, for $k = 0,1,2,\ldots$ until convergence, do

$$K_k \Delta x_k = F_k$$
$$x_{k+1} = x_k - \Delta x_k$$

Here, $F_k = F(x_k)$ is the load vector, $K_k = \partial_x F_k$ the stiffness matrix, and Δx_k a search direction to improve the current iterate x_k. Since the stiffness matrix is generally large, sparse, and indefinite for Augmented Lagrangian contacts, it is expensive to compute the search direction using direct methods such as LU-factorization. It is therefore tempting to try to use a cheaper iterative method for this purpose. We have implemented a Jacobian-Free Newton-Krylov (JFNK) method, which is a special variant of the well-known generalized minimal residual (GMRES) method.

Consider a single iteration with fixed k. Assuming no prior knowledge of the search direction Δx_k, our GMRES method uses an m-dimensional so-called Krylov space, defined by

$$\mathcal{V}_k^m = \{F_k, K_k F_k, K_k^2 F_k, \dots, K_k^{m-1} F_k\}$$

to construct a least squares approximation $\Delta\tilde{x}_k \in \mathcal{V}_k^m$ to Δx_k. To this end, the residual is required to be orthogonal to the next Krylov space $\mathcal{V}_k^{m+1} = K_k \mathcal{V}_k^m$, that is,

$$F_k - K_k \Delta\tilde{x}_k \perp \mathcal{V}_k^{m+1}$$

In practice this amounts to solving an $m+1$ by m least squares problem for m unknowns. The unspoken hope is, of course, that a good approximation can be obtained for a moderate value of m.

The unique feature with the JFNK method is that the involved Krylov spaces can be constructed without ever forming the stiffness matrix. Thus, allowing a very memory conserving method. The key observation is that matrix-vector multiplications of type Kv (with v denoting a generic vector), which are necessary for forming the Krylov vectors $\{K^j v\}_{j=0}^{m-1}$, can be interpreted as a directional derivative and computed as any finite difference, e.g.,

$$Kv = \frac{F(x + \epsilon v) - F(x)}{\epsilon}$$

where, typically, we use $\epsilon = 10^{-4} h$, with h a characteristic length. This formula can be iterated to compute all Krylov vectors in the Krylov spaces.

To accelerate convergence we (right) precondition the GMRES method using a stiffness matrix from the previous time step. This lagging avoids forming and LU factoring the matrix during every iteration.

3 Results

In this section, some examples of the Augmented Lagrange Method approach for Rigid Walls, Contact Entity and small-sliding contact are presented. The traditional application of rigid walls and contact entity is to replace a testing environment (like parts of a test rig, or the road surface in a crash analysis) with rigid, parametrized entities. This can save modelling time and reduce element count in the model.
All results in this section are obtained using the implicit solver of LS-DYNA.

3.1 Taylor bar impact

One of the most classical applications of **`*RIGIDWALL`** is perhaps for replacing a rigid crash barrier, see for example Ref. [5]. As an example of this, the Taylor bar impact analysis [2], is presented, see Fig. 2 for a comparison of the rigid wall reaction forces to previous implicit implementation and explicit (which should be seen as the reference solution in this case). It can be noted that the previous penalty method (blue curve in Fig. 2) misses the initial force peak, while the augmented Lagrange method follows the trend from the explicit (reference) solution.

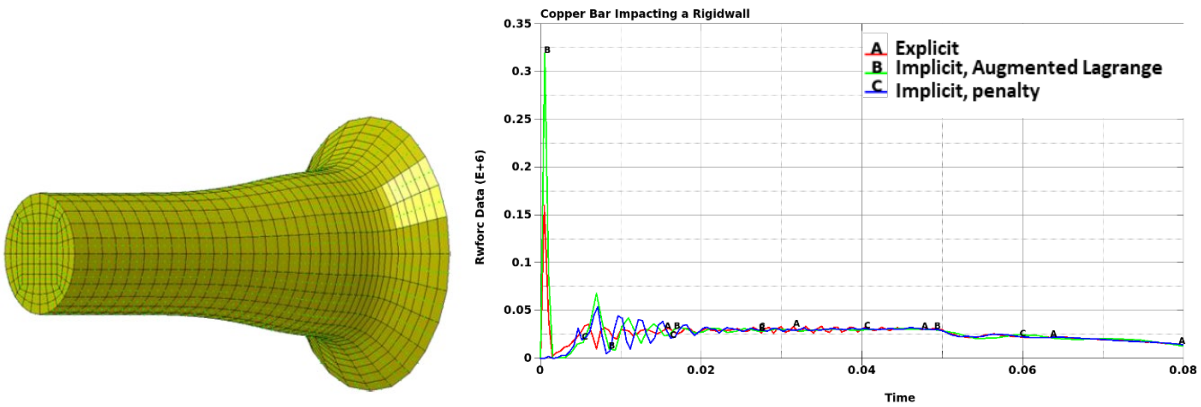

Fig.2: The left image shows a cylinder impacting a rigid wall. The right image shows a comparison of the reaction forces for the explicit solution (red) and the implicit solution using both the penalty method (blue) and the augmented Lagrange formulation (green).

3.2 Tensile testing of a LEGO® element

This example from LEGO® shows a tensile test of a LEGO® element. Two steel pins clamp the element, the lower is stationary and the upper is moved, while the reaction forces are measured. In this case, the steel pins are modelled as moving cylindrical rigid walls, with non-zero friction, shown as grey in Fig. 3, where the element is shown in orange. The simulation is performed using implicit dynamics. The final deformation is shown in the right image of Fig 3. The reaction forces are shown in Fig. 4. In this case, the ALM gives higher reaction forces, since the default settings of the penalty formulation results in quite large penetrations for this specific combination of mesh size and material properties. For this case, using the full-Newton solution method, 14338 iterations are required to complete the solution, while the JFNK method requires 3446 iterations. This is also reflected in the solution time, which is about 4 times faster for JFNK than BFGS.

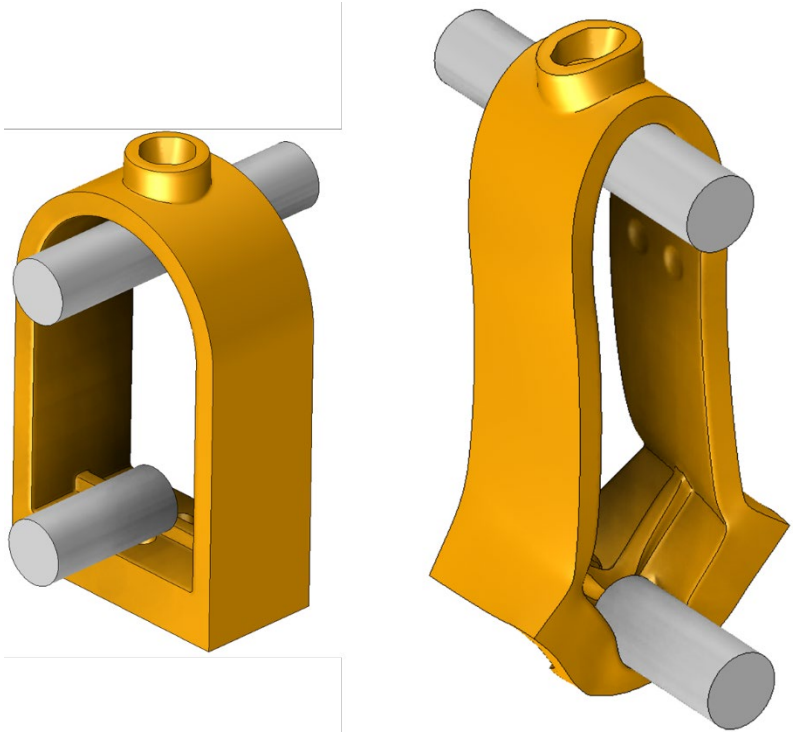

Fig.3: The left image shows the LEGO® element (orange) in the undeformed configuration, with the test rig as cylindrical rigid walls (grey). The right image shows the final configuration.

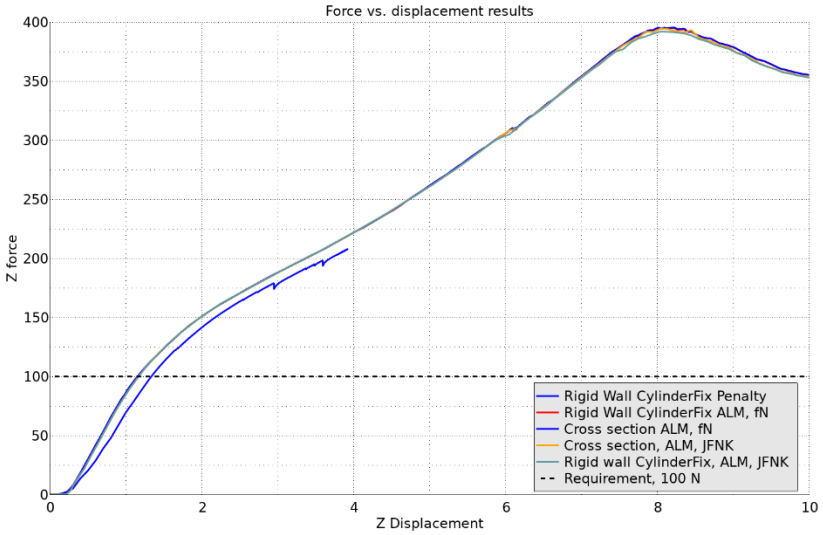

Fig.4: Reaction force in the moving cylinder (rigid wall) compared to section force and requirement of 100 N, for the different implementations. The simulation using the penalty method was aborted due to the extremely long solution time.

3.3 Prismatic indenter on a rubber block

A prismatic indenter (20×20×120 mm) is pushed into a rubber cube (100×75×75 mm), see the left image of Fig. 5. The target motion is 50 mm. The material model **`*MAT_HYPERELASTIC_RUBBER`** is used for the rubber, with C10 = 0.5508, C01 = 0.1377 and ν = 0.4995, which roughly corresponds to hardness 63 Shore-A. The indenter is modelled as moving prismatic rigid wall (keyword: **`*RIGIDWALL_GEOMETRIC_PRISM_MOTION_DISPLAY_ID`**). The coefficient of friction between the indenter and the rubber block was 0.1. The simulation is performed using implicit dynamics. The final configuration, using the ALM implementation, is shown in the right image of Fig. 5. The crossed edges that may be noted are since rigid walls use a one-way nodes-to-surface contact search, where only the tracked nodes are checked.

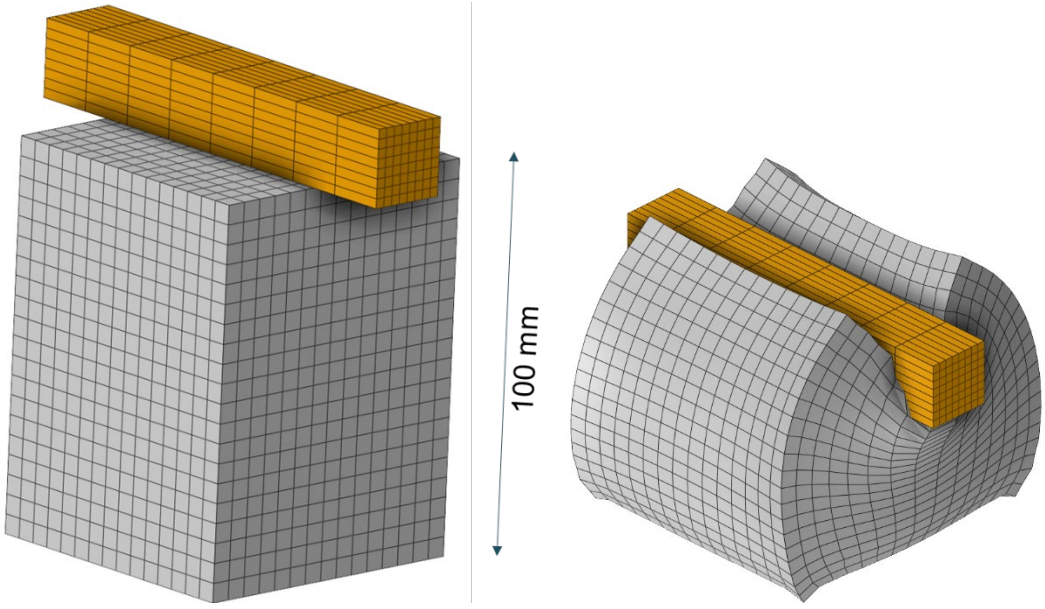

Fig.5: The left image shows the initial configuration of the indentation test. The grey part is the rubber block, and the orange part is the geometric representation of the prismatic rigid wall, auto-created by LS-DYNA. The right image shows the final configuration using the ALM implementation.

The simulation results using the ALM implementation of the rigid wall was compared to the penalty implementation of mpp/LS-DYNA R12.2.1. Initially, the penalty implementation works quite well, but for the final phase of the large indentation (after 48.4 mm) the reaction force drops due to an unstable

deformation mode, see Fig. 6. In this case, using the ALM for the rigid wall, the JFNK solution scheme requires totally 439 iterations to complete the 50 mm loading, while the standard BFGS solution scheme requires 6 times more (or 2677) iterations.

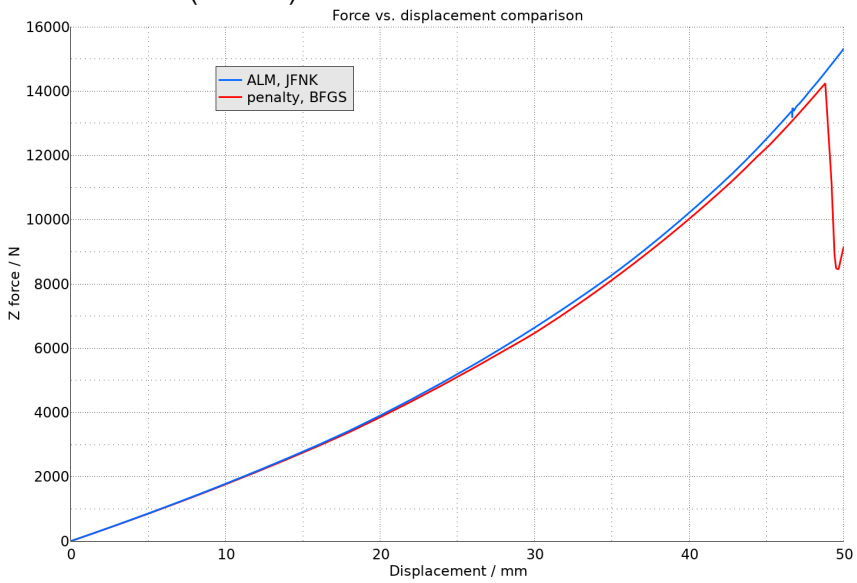

Fig.6: Comparison of rigid wall reaction force vs. displacement for the ALM and the penalty method. Quite good agreement is obtained, but for the last phase of compression, the penalty method loses contact force.

3.4 Three-point bending of a B-pillar

In this example, rigid walls are used for quickly and conveniently creating a simplified representation of a three-point bending rig. The B-pillar, taken from Ref. [5], is placed on prismatic supports, and the impactor is modelled as a cylindric moving rigid wall, see the top image of Fig. 7. The distance between the supports is approximately 805 mm. To determine the ultimate strength of the B-pillar, a prescribed displacement of 100 mm is applied to the cylindrical rigid wall. A friction coefficient of 0.1 is used with all the rigid walls. The simulation is performed using implicit dynamics. For this example, the JFNK method requires 7398 iterations and 9 retries to complete the solution, while the BFGS method requires 16849 iterations and 74 retries. Especially with regards to the significant reduction of retries, the JFNK method seems beneficial in this case.
The force vs. displacement curve is shown in Fig. 8. Similar results are obtained for all studied implementations.

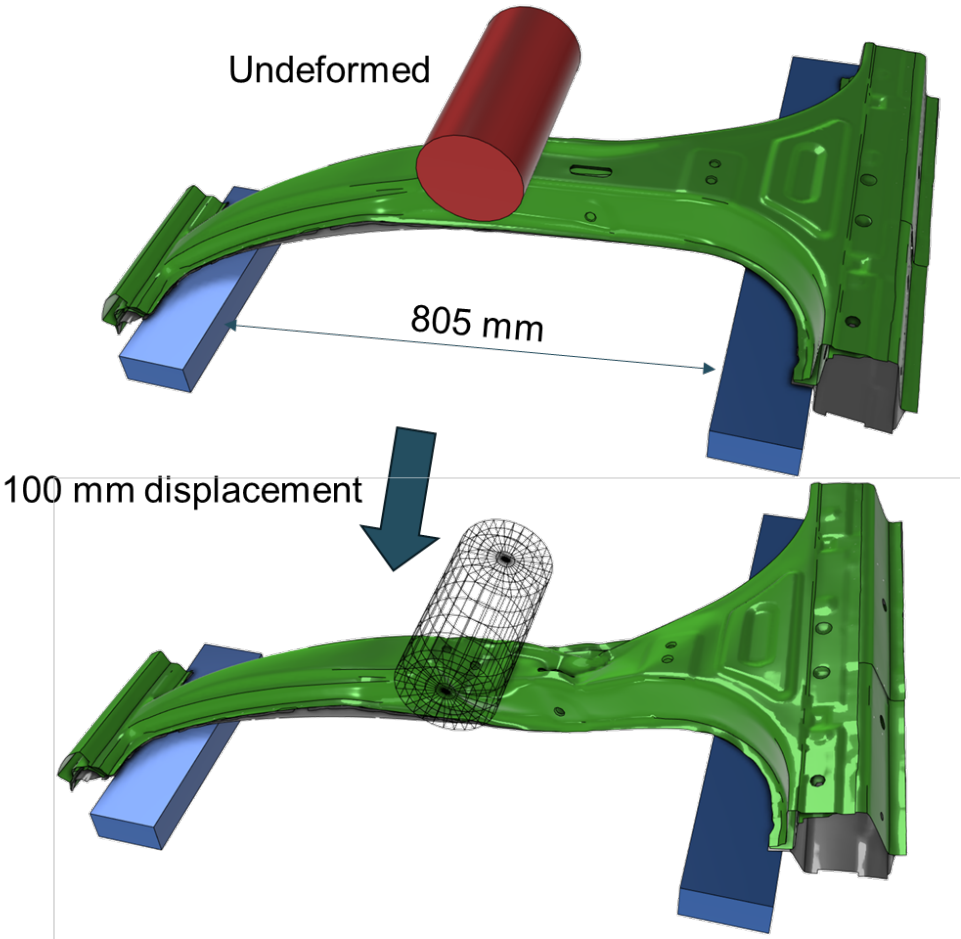

Fig.7: The top image shows the undeformed configuration. The blue prisms are fixed while the red cylindrical rigid wall is pushed 100 mm downwards, to obtain the final configuration, as shown in the bottom image.

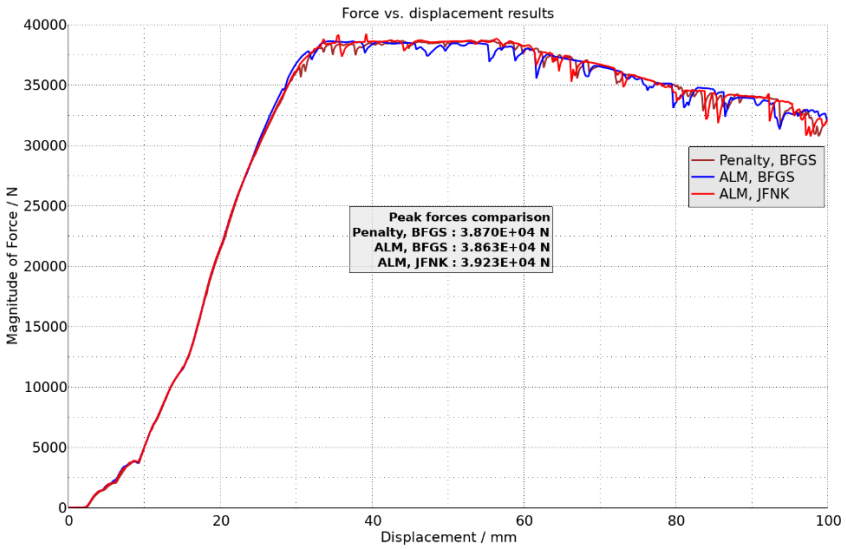

Fig.8: Force vs. displacement results for the different rigid wall implementations. Similar results for all rigid wall implementations and solution methods.

3.5 Spherical indenter on a rubber block

For the contact entity functionality (keyword: ***CONTACT_ENTITY**), this test demonstrates the capability to handle rolling contact with relatively high friction and large displacements. A spherical contact entity is first pressed 40 mm into a 100 mm high rubber block (using the same material model as in Section

3.2) and then translated in a spiral-like pattern by prescribed motions, while the rotational degrees-of-freedom are free. The coefficient of friction between the sphere and the rubber block is 0.45. The initial geometry is shown in the left image of Fig. 9, while an intermediate deformed state is shown in the right image. The trace line shows the trajectory of the north pole of the sphere.

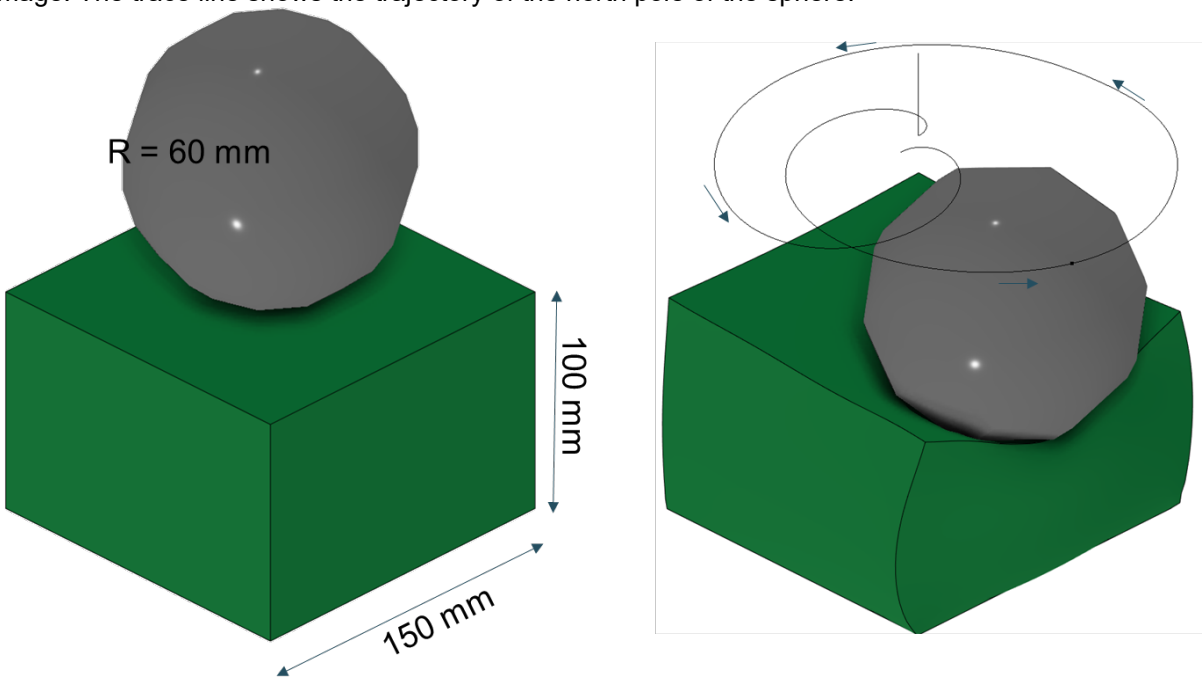

Fig.9: The left image shows the geometry of the sphere (grey) and the rubber block (green). The right image shows an example of the deformed shape during the rolling phase, with the black line showing the trajectory of the north pole of the sphere.

3.6 Oil-canning of a door panel

In this example, a spherical contact entity is used to model the indenter in an oil-canning test of a door panel, see Fig. 10. The FE-model of the door is taken from Ref. [5]. The indenter (R=25 mm) is pushed 50 mm into the door panel, in the transverse (Y) direction by a prescribed motion, and then translated back to the original position. The simulation is performed using implicit statics, and the standard BFGS solution method. The force vs. displacement results are compared to results using a meshed rigid sphere and Mortar contact in Fig.11. In this case, the solution time for the contact entity is even 15 % less than for the simulation using a meshed rigid part and Mortar contact (using the same hardware and other settings).

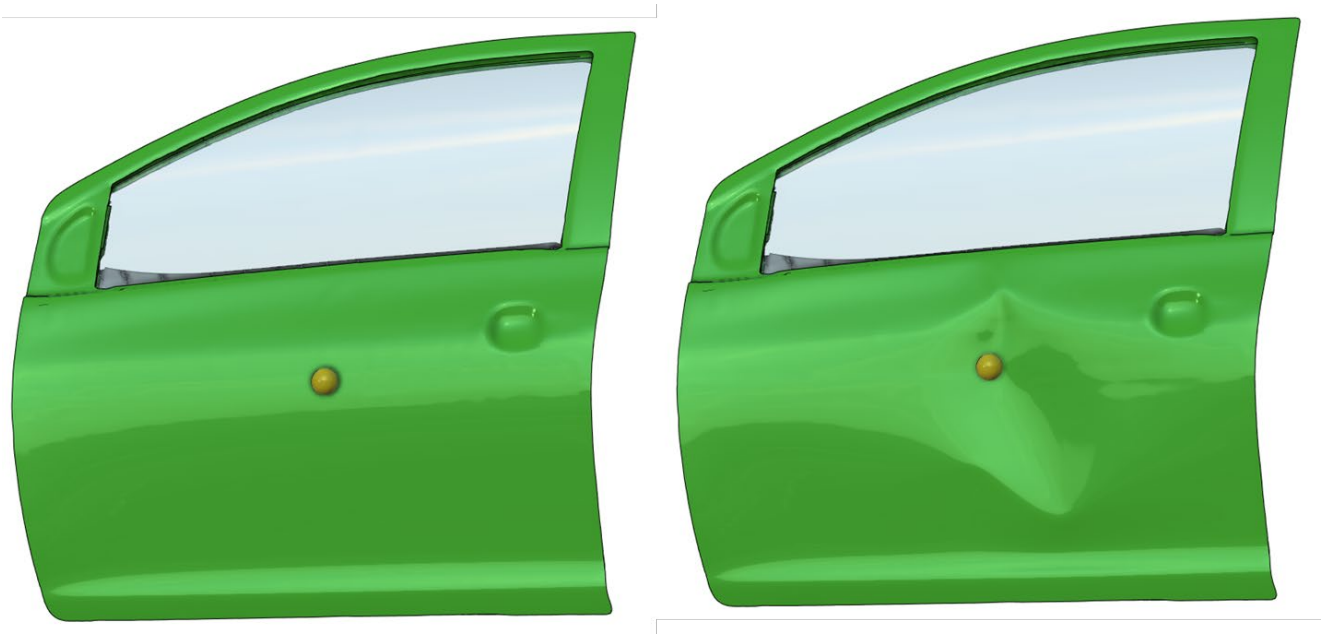

Fig.10: The left image shows the initial geometry of the door with the spherical indenter. The right image shows the deformed shape after 50 mm indentation and release.

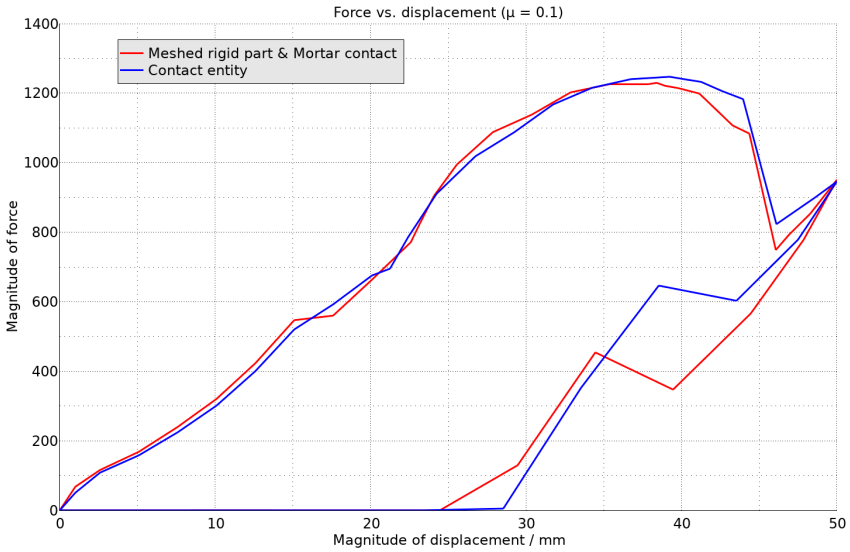

Fig.11: Force vs. displacement results for the contact entity compared to the meshed rigid part.

3.7 Bolt pre-tension of an L-bracket assembly

To demonstrate the small-sliding constraint contacts in an example, the assembly of an L-bracket to a base plate using four bolts is studied, see the left image of Fig. 12. The assembly is subjected to 1 kN loading/unloading first in the transverse (X) and then in the longitudinal (Y) direction, but first bolt pre-tensioning is applied. The objective of the analysis is to determine the peak stress in the bracket. This is a simple but typical example of where small-sliding contacts may be well motivated. After bolt pre-tension is applied, and at this loading (1 kN), no sliding is expected between the parts in the assembly. Using constraint contacts and the JFNK solution method, 177 iterations are required to complete the solution statistics, compared to 229 iterations using Mortar contact and the standard BFGS solution method. The peak stress in the L-bracket is computed as 297 MPa using the constrained contact, while the Mortar result is 321 MPa (8 % higher). Solution times are comparable.

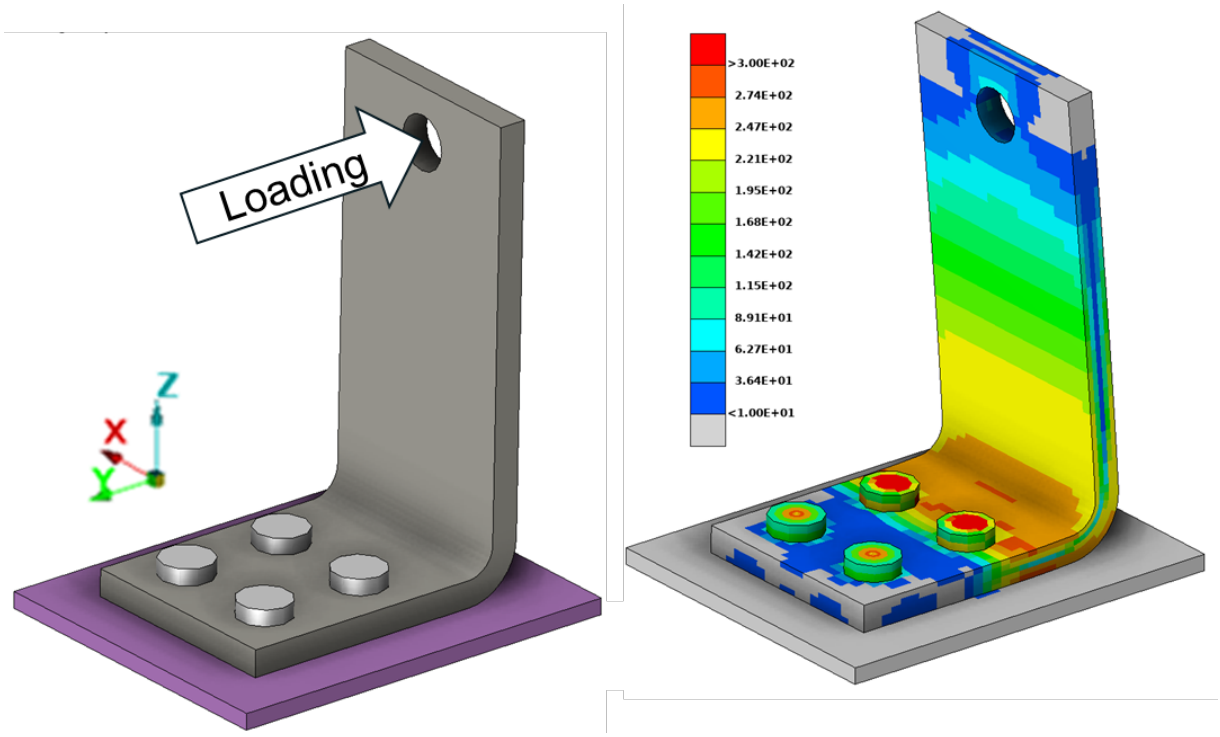

Fig.12: The left image shows the geometry of the L-bracket assembly. The loading is applied to a distributing coupling (`*CONSTRAINED_INTERPOLATION`) at the top bolt hole. The right image shows the stress corresponding to the peak loading.

4 Summary and outlook

For implicit analyses, the Lagrange multiplier approach to rigid walls and analytical rigid shapes (**`*CONTACT_ENTITY`**) will replace the previous implementation of these features. The examples of Section 3 demonstrate that the present implementations are useful for different applications, like creating simplified representations of test rigs. Further developments will be driven by customer input and requests. The present implementation of the rigid walls is based on node-to-surface penetration check, which means that some contact situations may be missed, like edge-to-edge or edge-to-surface contacts. In future versions, an extension to (optionally) segment-based contact search for rigid walls and contact entities may be considered.

The development of constraint-type contacts for implicit analyses, possibly extending the functionality to large sliding, will continue based on customer input. We believe that in for example process simulations, like extrusion of plastics or forming of carton packages, the use of augmented Lagrange contacts may deliver results even closer to reality, since the details of the tooling may be challenging to fully resolve using a penalty method. Some further developments will be required to make the contacts useful in, for example coupled thermomechanical simulations.

Also, further research on the alternative JFNK methods to improve the nonlinear solver for handling the saddle-point type of problems associated with the Lagrange multiplier approach will be required. Results so far, for the rigid walls especially, seem promising, regarding rate of convergence and iteration count.

5 Literature

[1] Borrvall, T., "Mortar contact algorithm for implicit stamping analyses in LS-DYNA ", 10th International LS-DYNA conference, 2008

[2] Wilkins, M. L., and Guinan, M. W., “Impact of cylinders on a rigid boundary”, Journal of Applied Physics, 1973, **44**:1200-1206

[3] Knoll, D., and Keyes, D., “Jacobian-free Newton-Krylov method: A survey of approaches and applications”, Journal of Computational Physics, 2004, **193**:357-397

[4] Renard, Y., “Generalized Newton’s methods for the approximation and resolution of frictional contact problems in elasticity”, Computer Methods in Applied Mechanics and Engineering, 2003, **256**:38-55s

[5] Internet source: https://www.ccsa.gmu.edu/models/2010-toyota-yaris/

[6] Internet source: 2010 Toyota Yaris Finite Element Model Validation Detailed Mesh, Presentation, doi:10.13021/G8CC7G